Journal of Physics: Conference Series **706** (2016) 042001 doi:10.1088/1742-6596/706/4/042001

CP violation in charmless $B^{\pm}$ three-body decays: where Flavour Physics meets Hadron Physics

Alberto C. dos Reis, on behalf of the LHCb collaboration.
Centro Brasileiro de Pesquisas Físicas - CBPF, Rio de Janeiro, Brazil
E-mail: alberto@cbpf.br

Abstract. In this work a study of the *CP* asymmetry across the phase space of charmless three-body decays of $B^{\pm}$ mesons is presented. Four final states containing only charged light mesons are considered: $\pi^-\pi^-\pi^+$, $K^-\pi^-\pi^+$, $K^-\pi^-K^+$ and $K^-K^-K^+$. The observed pattern of the *CP* asymmetry distribution suggests the action of different mechanisms generating strong phases, which are necessary to give rise to *CP* violation.

1. Introduction

The Standard Model (SM), one of the pilars of the contemporary Physics, is challenged by several observations, including the baryon asymmetry in the Universe (BAU).

The phenomenon of *CP* violation (*CP*V) is one of the Sakharov [1] conditions that are necessary to explain the baryogenesis. *CP* violation arises in the SM due to an irreducible phase in the Cabibbo-Kobayashi-Maskawa (CKM) matrix. So far, all measurements of *CP* violation in decays of flavoured mesons are consistent with the SM predictions. However, the amount of *CP*V contained in the CKM matrix is orders of magnitude smaller than that required to explain the BAU, implying that other sources of *CP*V must exist. The study of *CP*V is therefore a portal to new Physics.

There are three possible manifestations of *CP*V in decays of a flavoured mesons M:

- a difference in the decay rate of a meson and its antiparticle, usually refered to as *CP*V in the decay, possible for both $M^{\pm}$ and M^0;
- a difference in the oscillation frequency between a meson and its antiparticle, usually refered to as *CP*V in the mixing, possible only for M^0;
- a mismatch between the relative phases of mixing and decay amplitudes of a meson and its antiparticle, also possible only for M^0.

In this work we study the first type of *CP*V using decays of $B^{\pm}$ mesons into three light mesons. Given that mixing is not possible for charged B mesons, its charmless decays are an excellent laboratory for *CP*V in decay.

*CP*V in decay arises from the interference between amplitudes with different weak and strong phases leading to the same final state:

$$A = a_1 + a_2\, e^{(\delta+\gamma)}, \quad \overline{A} = a_1 + a_2\, e^{(\delta-\gamma)}\ ,$$

where γ and δ are the weak (CP odd) and strong (CP even) phases and a_1 and a_2 are real numbers. Given that $\Gamma(\bar{B} \to f) \propto |A|^2$ and $\Gamma(\bar{B} \to \bar{f}) \propto |\overline{A}|^2$, the $\mathcal{A}_{CP}^{\rm dir}$ observable is

$$\mathcal{A}_{CP} \equiv \frac{\Gamma(B \to f) - \Gamma(\bar{B} \to \bar{f})}{\Gamma(B \to f) + \Gamma(\bar{B} \to \bar{f})} = \frac{2a_1 a_2 \sin\gamma \sin\delta}{a_1^2 + a_2^2 + 2a_1 a_2 \cos\gamma \cos\delta}.$$

This is realized in the context of the Bander-Silverman-Soni (BSS) mechanism [2], illustrated in Fig. 1. The diagrams show two amplitudes for the $B^+ \to K^+\pi^+\pi^-$ decay (charge conjugation is implict, unless otherwise stated). The tree amplitude is proportional to V_{ub}, having therefore the weak phase γ, and no strong phase. The penguin amplitude, on the other hand, has no weak phase, if the quarks in the loop are either a c or a t quark. In their paper, Bander, Silverman and Soni showed that a strong phase could be generated when the c quarks in the penguin amplitude are on shell. For two-body decays, this would be the only source of the necessary strong phase difference.

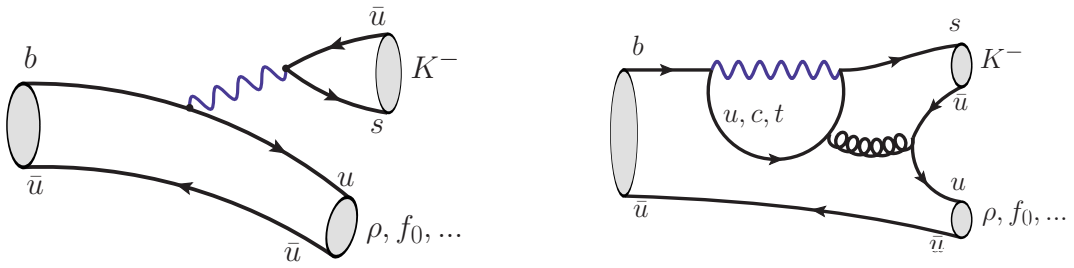

Figure 1. Tree and penguin diagrams for the $B^- \to K^-\pi^-\pi^+$ decay.

Two aspects make three-body decays particularly interesting. Firstly, three-body decays have a two-dimensional phase space, allowing one to search for local effects. The second aspect is that most final states have a rich resonant structure. The interference between resonances as well as final state interactions (FSI) at hadron level may provide additional sources of strong phase difference. These phase difference vary across the phase space and can be very large, giving rise to large CP asymmetries in regions of the Dalitz plot.

In this work we discuss the results of the CP violation search in the Dalitz plot of the decays $B^+ \to \pi^+\pi^+\pi^-$, $B^+ \to K^+\pi^+\pi^-$, $B^+ \to K^+\pi^+K^-$ and $B^+ \to K^+K^+K^-$ with data collected by the LHCb experiment. The results correspond to the full Run I data set (3 fb^{-1}) [3].

2. Sample selection

The three tracks from the $B^\pm$ decay candidate are required to form a good quality secondary vertex with a significant separation from the associated primary vertex (PV) from the pp interaction. The reconstructed B candidate momentum has to point back to the PV. The four channels, $B^\pm \to K^\pm h^+ h^-$ and $B^\pm \to \pi^\pm h^+ h^-$ ($h = \pi,\ K$) are topologically and kinematically similar. The same selection criteria are used for all four modes, except for the particle identification requirements, which are specific to each final state. Charm meson contributions are removed by explicit mass vetoes. A multivariate analysis (Boosted Decision Tree - BDT) is performed to reduce the combinatorial background. The cut on the BDT discriminating variable is chosen to maximise the ratio $S/\sqrt{S+B}$, where S and B represent

Table 1. Signal yields of charmless three-body $B^{\pm}$ decays for the full LHCb dataset.

Decay mode	Yield
$K^+\pi^+\pi^-$	$181\,074 \pm 556$
$K^+K^+K^-$	$109\,240 \pm 354$
$\pi^+\pi^+\pi^-$	$24\,907 \pm 222$
$K^+\pi^+K^-$	$6\,161 \pm 172$

the expected number of signal and background candidates within the signal region. Particle identification reduces the contamination from the cross-feed from other B decays to a small level.

The invariant mass spectra of the selected $B^{\pm}$ candidates are shown in Fig. 2. Unbinned extended maximum likelihood fits to the mass spectra of the selected candidates are performed separately for each channel to obtain the signal yields and raw asymmetries.

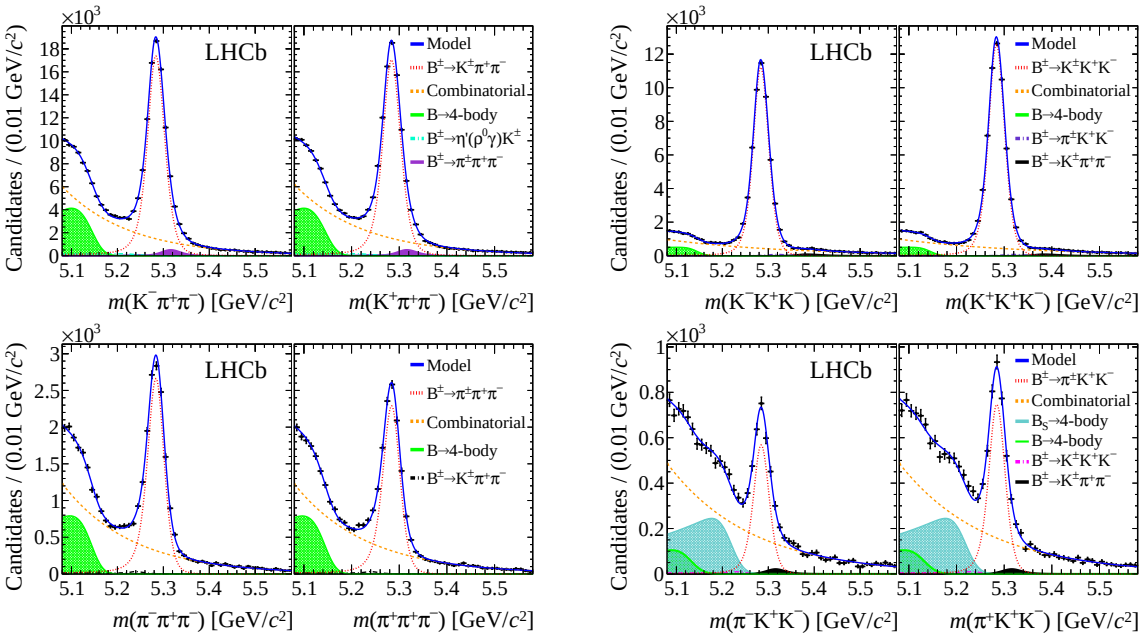

Figure 2. Invariant mass spectra of (top left) $K^+\pi^+\pi^-$, (top right) $K^+K^+K^-$, (bottom left) $\pi^+\pi^+\pi^-$ and (bottom right) $K^+\pi^+K^-$ decays. The left panel on each figure shows the B^- candidates and the right panel shows the B^+ candidates. The results of the unbinned maximum likelihood fits are overlaid. The main components of the fits are also shown.

The Dalitz plots for the various final states are shown in Fig. 3. In all cases a dense, rich resonant structure is observed at low $\pi^+\pi^-$, $K^+\pi^-$ and K^+K^- invariant mass squared. Since the phase space is so large, in all cases there is also a significant nonresonant component.

3. *CP* asymmetry across the Dalitz plot

The raw charge asymmetry is computed from observed signal yields:

$$A_{\rm obs} = \frac{N_{B^-} - N_{B^+}}{N_{B^-} + N_{B^+}}.$$

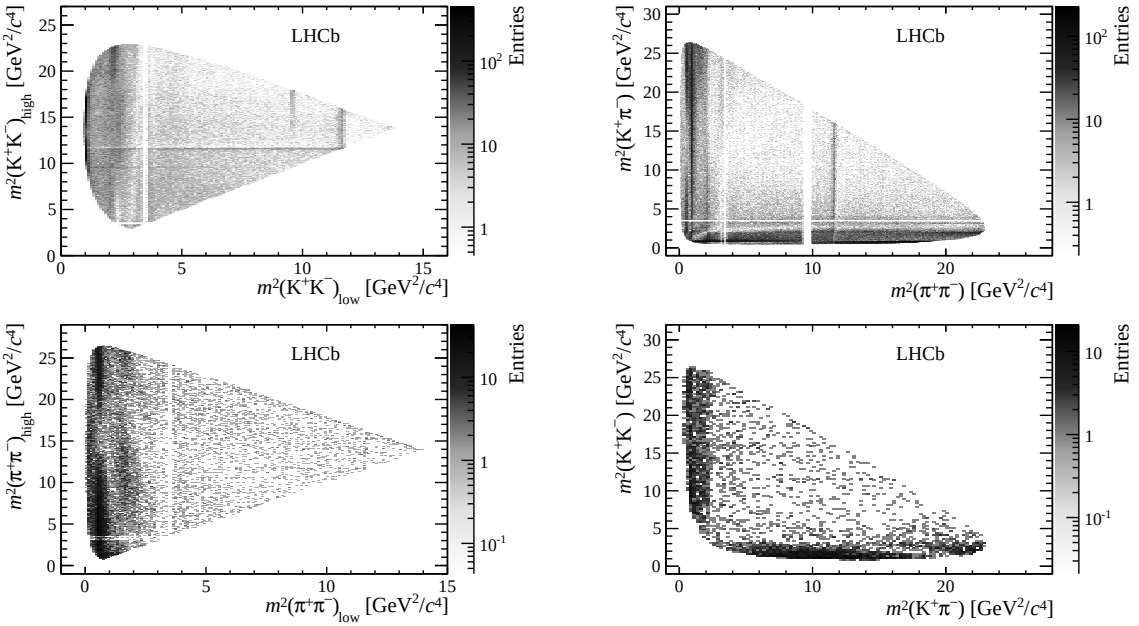

Figure 3. Dalitz plots of (top left) $K^+K^+K^-$, (top right) $K^+\pi^+\pi^-$, (bottom left) $\pi^+\pi^+\pi^-$ and (bottom right) $K^+\pi^+K^-$ candidates.

The *CP* asymmetry is obtained correcting $A_{\rm obs}$ for the $B^\pm$ production asymmetry and asymmetry in the detection of unpaired hadrons ($B^\pm \to K^\pm h^+h^-$, $B^\pm \to \pi^\pm h^+h^-$),

$$\mathcal{A}_{CP} = A_{\rm obs} - A^B_{\rm prod} - A^h_{\rm det} \ .$$

The correction factors $A^B_{\rm prod}$ and $A^h_{\rm det}$ are determined using data-driven methods. Typical values are of the order of 1%, and are small compared to $A_{\rm obs}$. In all plots that follow we assume $A_{\rm obs} \simeq \mathcal{A}_{CP}$.

The Dalitz plots of the four channels are divided into bins with same population. In each bin the value of $\mathcal{A}_{CP}$ is computed. The distribution of $\mathcal{A}_{CP}$ values is shown in Fig. 4.

There are several interesting features in the distribution of $\mathcal{A}_{CP}$ across the Dalitz plots. In some regions one observes *CP* asymmetries of 80%, a rather surprising result. In the $K^+K^+K^-$ and $K^+\pi^+K^-$ final states the asymmetry is mostly negative, whereas in the $K^+\pi^+\pi^-$ and $\pi^+\pi^+\pi^-$ channels the asymmetry is both positive and negative.

4. *CP* asymmetry and $\pi\pi \leftrightarrow KK$ rescattering

A zoom of the low mass regions of the $B^\pm \to K^\pm h^+h^-$ is shown in Fig. 5. The *CP* asymmetry in the regions limited by the red vertical lines have opposite signs in the two channels, especially if one is restricted to the lower half of the Dalitz plot ($m^2_{hh} < 20$ GeV$^2/c^4$).

A possible interpretation of this pattern invokes *CPT* invariance. *CPT* symmetry imposes a constraint on the particle/antiparticle partial widths: in a family of final states sharing the same quantum numbers one must have $\sum \Gamma_i(B \to f_i) = \sum \Gamma_i(\overline{B} \to \bar{f}_i)$. The $\pi\pi$ interaction becomes inelastic with the opening of the $K\overline{K}$ channel, and up to a center-of-mass energy of ~ 1.5 GeV (the regions limitated by the red lines) all the inelasticity of the $\pi\pi$ interaction goes into the $K\overline{K}$ channel. Hereafter the region between the two red lines in Figs. 5 and 6 ($1 < m^2_{h^+h^-} < 2.2$ GeV$^2/c^4$) will be referred to as the rescattering region.

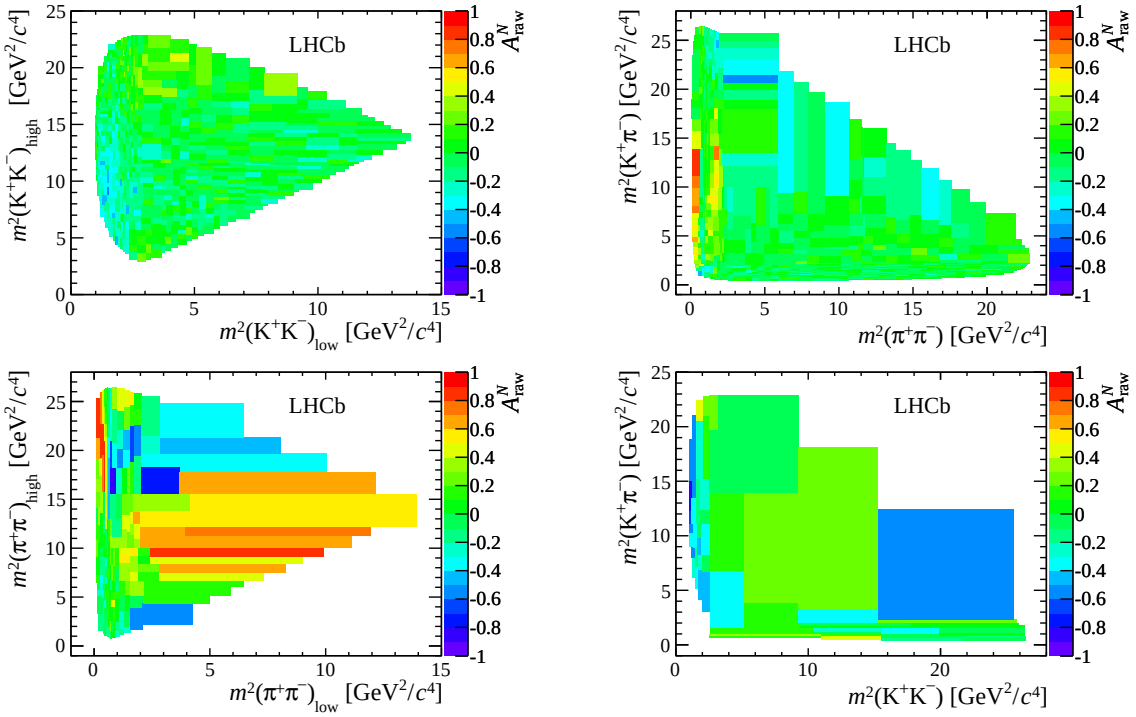

Figure 4. Measured $A_{\rm obs}$ in Dalitz plot bins of background-subtracted and acceptance-corrected events for (top left) $K^+K^+K^-$, (top right) $K^+\pi^+\pi^-$, (bottom left) $\pi^+\pi^+\pi^-$ and (bottom right) $K^+\pi^+K^-$ decays.

The $K^+\pi^+\pi^-$ and $K^+K^+K^-$ channels are therefore connected by final state interactions (FSI). In the absence of *CP* violation there would be a balance between the outgoing and the ingoing flux in each channel. But if *CP* is violated this balance would be broken, giving rise to a positive asymmetry in one channel which must be compensated by a negative asymmetry in the other channel. Of course a comprehensive analysis of such effect requires the inclusion of neutral modes ($\pi^0\pi^0$ and $K^0\overline{K}^0$). But if this is the underlying mechanism of the observed *CP* asymmetries, then the $\pi\pi \leftrightarrow KK$ rescattering would provide the source of the strong phase difference, a unique feature of multi-body decays.

A similar effect is observed in the $B^\pm \to \pi^\pm h^+h^-$ channels, as shown in Fig. 6. The asymmetry in the rescattering region is more dramatic in the $K^+\pi^+K^-$ channel, since its resonant structure is more simple than that of the $\pi^+\pi^+\pi^-$. In the latter one sees other mechanisms in action.

The values of the *CP* asymmetry for events in the rescattering region are summarized in Table 2. The corresponding mass spectra are shown in Fig. 7.

Table 2. *CP* asymmetries in the rescattering region

Decay	signal yield	$\mathcal{A}_{CP}$
$B^\pm \to K^\pm\pi^+\pi^-$	15562 ± 165	$+0.121 \pm 0.022$
$B^\pm \to K^\pm K^+K^-$	16992 ± 142	-0.211 ± 0.014
$B^\pm \to \pi^\pm\pi^+\pi^-$	4329 ± 76	$+0.172 \pm 0.027$
$B^\pm \to \pi^\pm K^+K^-$	2500 ± 57	-0.328 ± 0.041

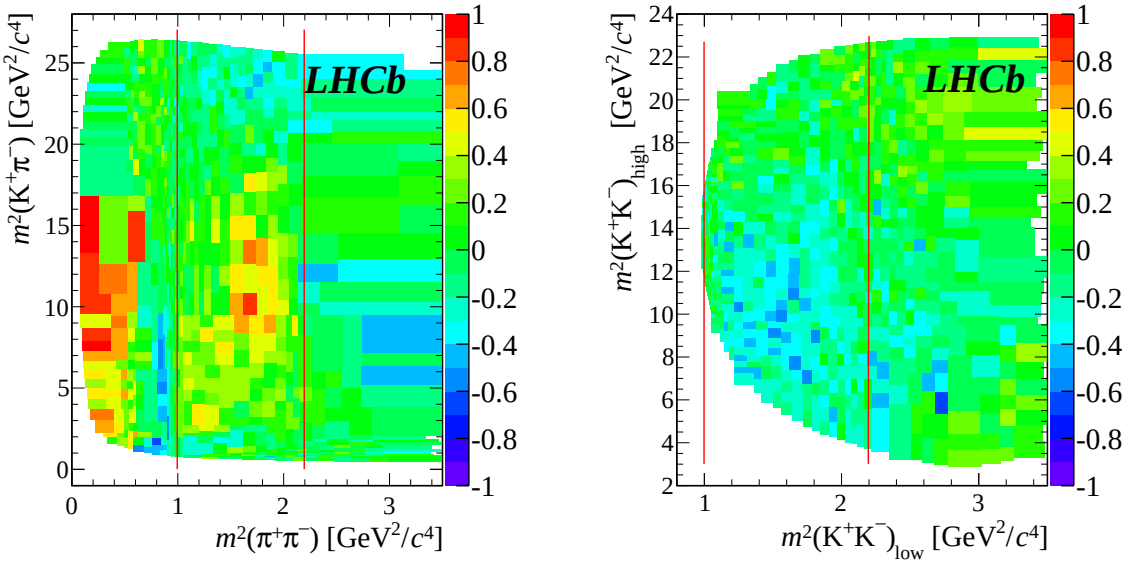

Figure 5. A zoom of the Dalitz plot of the $K^+\pi^+\pi^-$ (left) and $K^+K^+K^-$ (right), showing the distribution of $\mathcal{A}_{CP}$. The red vertical lines indicate the kinematic region where $\pi^+\pi^- \to K^+K^-$ rescattering is allowed.

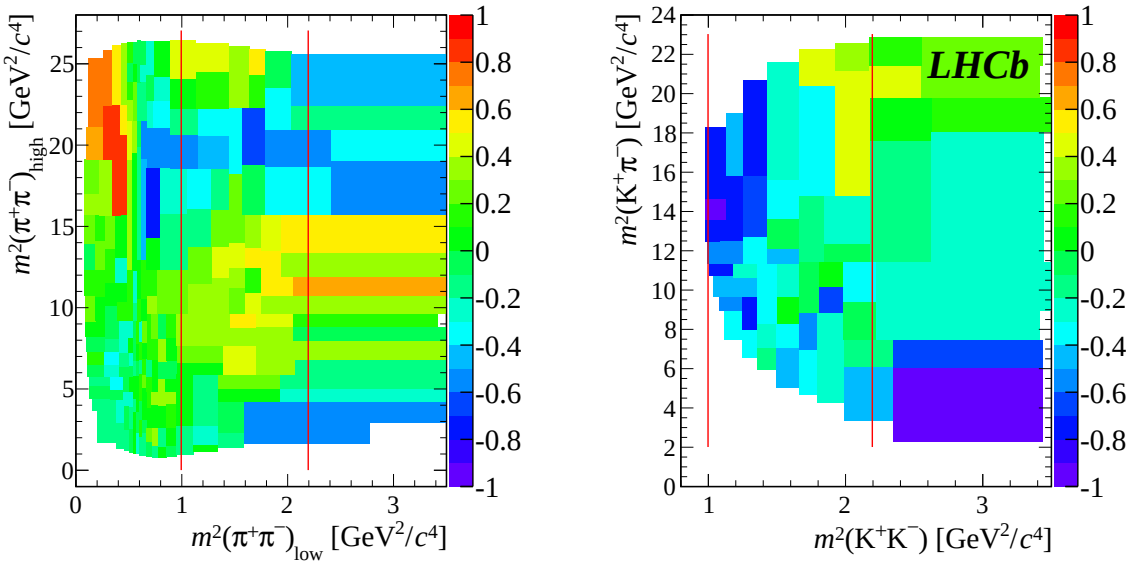

Figure 6. A zoom of the Dalitz plot of the $\pi^+\pi^+\pi^-$ (left) and $K^+\pi^+K^-$ (right), showing the distribution of $\mathcal{A}_{CP}$. The red vertical lines indicate the kinematic region where $\pi^+\pi^- \to K^+K^-$ rescattering is allowed.

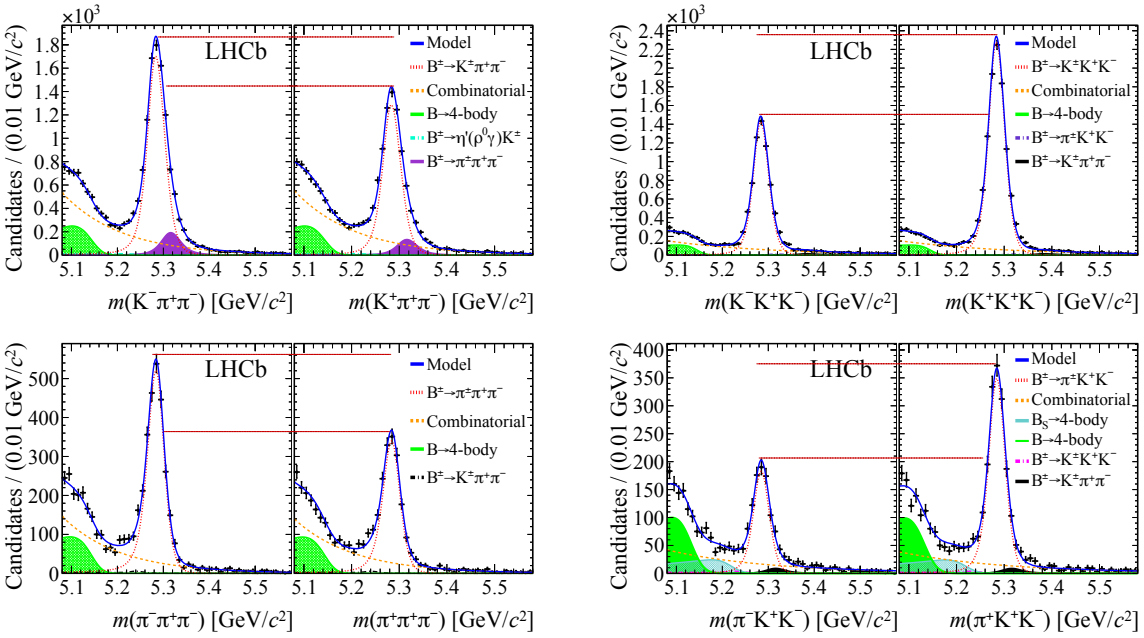

Figure 7. Invariant mass distributions in the rescattering regions for $K^+\pi^+\pi^-$ (top left), $K^+K^+K^-$ (top right), $\pi^+\pi^+\pi^-$ (bottom left), and $K^+\pi^+K^-$ (bottom right) decays. The left panel in each figure shows the B^- candidates and the right panel shows the B^+ candidates.

5. *CP* asymmetry and resonance interference

Another interesting pattern is observed in the $K^+\pi^+\pi^-$ and $\pi^+\pi^+\pi^-$ channels, which are those having a rich resonant structure. The In Figs. 5 and 6 (plots on the left) regions with very large $\mathcal{A}_{CP}$ can be observed below 1 GeV$^2/c^4$. As one moves from threshold to the first red line a sudden change in the sign of $\mathcal{A}_{CP}$ is clearly visible.

This effect may be caused by the interference between the various resonances. In order to investigate this possibility, the low $\pi^+\pi^-$ invariant mass region of the $B^+ \to \pi^+\pi^+\pi^-$ Dalitz plot is divided into four zones, as shown in Fig. 8. The vertical line dividing zones I and III from zones II and IV is at the $\rho(770)$ mass, whereas the horizontal line separating zones I and II from zones III and IV is at the position where the cosine of the helicity angle θ is zero. The helicity angle is defined as the angle between the two like-charge pions in the $\pi^+\pi^-$ rest frame.

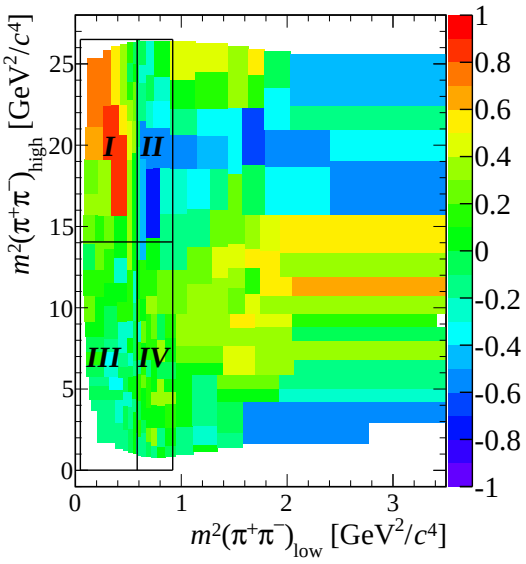

Figure 8. A zoom of the low $\pi^+\pi^-$ invariant mass from the $B^+ \to \pi^+\pi^+\pi^-$ decay, showing the region $m\pi^+\pi^-_{\rm low} < 1$ GeV$^2/c^4$ divided into four zones.

A simple decay model is built, having only two contributions, namely the $\rho\pi^+$ and a uniform, nonresonant amplitude . The $\rho\pi^+$ amplitude is represented by a product of form factors for the B and ρ decays, a Breit-Wigner function describing the ρ lineshape and an angular function,

$$A_\rho = \frac{F_D F_\rho}{s_{\rm low} - m_\rho^2 + i m_\rho \Gamma} \, |\mathbf{p}||\mathbf{q}| \cos\theta \equiv f_\rho (s_{\rm low} - m_\rho^2 - i m_\rho \Gamma) \cos\theta, \tag{1}$$

where m_ρ is the nominal ρ mass and $\mathbf{p}, \mathbf{q}$ are the momenta os the two like-charge pions.

The decay amplitude for the B^+ and the B^- decays are

$$\mathcal{M}_\pm(s_{\rm low}, s_{\rm high}) = c_\pm^\rho A_\rho + c_\pm^{\rm NR}, \tag{2}$$

where $c_\pm^\rho$ and $c_\pm^{\rm NR}$ are complex constants.

Since the number of decays of each charge type is proportional to the modulus squared of the decay amplitudes, the *CP* asymmetry is

$$\mathcal{A}_{CP}(s_{\rm low}, s_{\rm high}) \propto |\mathcal{M}_-|^2 - |\mathcal{M}_+|^2, \tag{3}$$

Using eqs. (1), (2) and (3), one has

$$\mathcal{A}_{CP} \propto (c_-^{\rho\ 2} - c_+^{\rho\ 2})|A_\rho|^2 + (c_-^{\mathrm{NR}\ 2} - c_+^{\mathrm{NR}\ 2}) + \cos\theta\ (s_{\mathrm{low}} - m_\rho^2)\ 2\mathrm{Re}(c_-^\rho c_-^{\mathrm{NR}} - c_+^\rho c_+^{\mathrm{NR}}) f_\rho + \ldots \quad (4)$$

The term proportional to $\cos\theta$ in eq. (4) changes sign when s_{low} crosses the ρ mass (passing from zones I and III to zones II and IV). Moreover, in zones I and II $\cos\theta < 0$, whereas in zones II and IV $\cos\theta > 0$. The other terms have always the same sign. In this model one would have a positive $\mathcal{A}_{CP}$ below the ρ mass, and negative above it, with a zero at $s_{\mathrm{low}} = m_\rho^2$.

In Fig. 9 the low $\pi^+\pi^-$ invariant mass projection is shown, separately for B^+ and B^- events (left plot). The *CP* asymmetry is proportional to the difference between the B^+ and B^-yields (eq. (3)), which is shown in the plot on the right of Fig. 9. The pattern matches that expected by the simple model above, suggesting the interference between the resonant components to provide the strong phase difference required for the *CP* asymmetry to manifest.

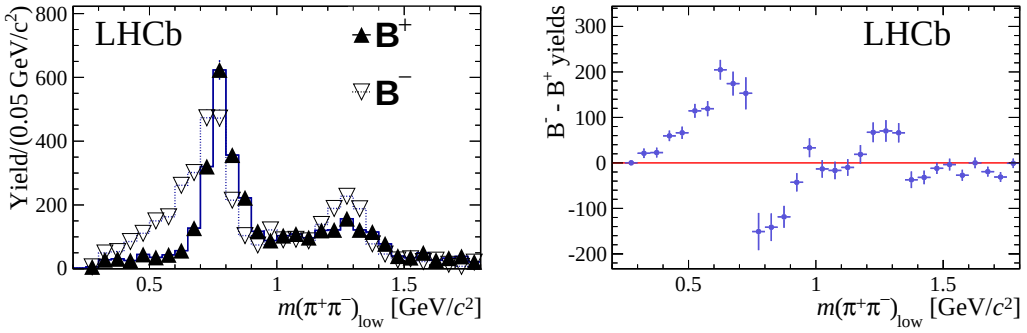

Figure 9. The low $\pi^+\pi^-$ invariant mass projection of the B^+ (full triangles) and B^- (open triangles) events from zones I and II (left plot); and the difference between the B^- and B^+ yields in bins of $m_{\pi^+\pi^-}$.

6. Conclusion

The study of *CP* violation in *B* decays reveals an unusual pattern with large asymmetries in specific regions of the Dalitz plot. Although a full amplitude analysis is the necessary step for a quantitative study of this phenomenon, the data suggests that one should take into account the hadronic degrees of freedom as the source of strong phase differences between amplitudes that lead to the same final state. In this respect, the study of the $\mathcal{A}_{CP}$ distribution across the Dalitz plot is an instance where Flavour Physics and Hadron Physics meet. A theoretical description the three-body FSI, rescattering, nonresonant components, is required in order to allow experimentalists to take full benefit of the large data sets available from the LHC experiments.

Acknowledgments

This work was supported by the Brazilian Conselho Nacional de Desenvolvimento Científico e Tecnológico - CNPq.

References

[1] A. D. Sakharov, *Violation of CP Invariance, C Asymmetry and Baryon Asymmetry of the Universe*, Journal of Experimental and Theoretical Physics (JETP) **5**, 32 (1967).

[2] M. Bander, D. Silverman and A. Soni, *CP Noninvariance in the Decays of Heavy Charged Quark Systems*, Phys. Rev. Lett. **43**, 242 (1979).
[3] LHCb collaboration, R. Aaij *et al.*, *Measurements of CP violation in the three-body phase space of charmless $B^{\pm}$ decays* Phys. Rev. **D** 90, 112004 (2014).